

# Experimental and Theoretical Validation of Ga<sub>2</sub>O<sub>3</sub> Thin Films Deposited by Physical Vapor Deposition

**Khue T. Lai\***, **Nafiseh Badiei\***, **Shuo Deng\***, **Petar Igić\*\***, and **Lijie Li\***

\*College of Engineering, Swansea University Bay Campus, Swansea, SA1 8EN, UK

{k.t.lai, n.badie, shuo.deng, l.li}@swansea.ac.uk

\*\*Institute for Future Transport and Cities, Coventry University, Coventry, CV1 5FB, UK

{ad1503}@coventry.ac.uk

*Abstract—In this work, we have shown that beta-gallium oxide (Ga<sub>2</sub>O<sub>3</sub>) thin films of differing thickness could be obtained by physical vapor deposition method, employing proper annealing conditions. These enable us to compare the variation of optical properties like transparency, band gap in these phases. Apart from these, our analysis of transmittance spectra of beta-Ga<sub>2</sub>O<sub>3</sub> indicated the reduction of structural disorders (amorphous to crystalline) with increase in annealing temperature. The calculated band gap based on Density Functional Theory (DFT) for bulk beta-Ga<sub>2</sub>O<sub>3</sub> thin films ~ 4.9 eV (direct) at room temperature is in excellent agreement with our experimentally measured values. This work will serve as design guidance for the new Ga<sub>2</sub>O<sub>3</sub> based thin film electronics.*

*Keywords—Density functional theory; gallium oxide; optical properties; physical vapor deposition; wide band gap semiconductors.*

## 1. Introduction

Wide band gap ( $E_g$ ) semiconductors such as gallium nitride (GaN), and silicon carbide (SiC) have been applied to field effect transistors, high electron mobility transistors and optoelectronics devices such as UV light-emitting diodes [1-2]. Compared with other wide  $E_g$  semiconductors like SiC ( $E_g \sim 3.3$  eV) and GaN ( $E_g \sim 3.4$  eV), beta-gallium oxide ( $\beta$ -Ga<sub>2</sub>O<sub>3</sub>) is a promising semiconductor due to its direct ultrawide  $E_g \sim 4.9$  eV, n type conductivity, high ultraviolet to visible transparency, excellent chemical and thermal stability in the high temperature range. This material possesses great potentials in achieving high power electronic and optoelectronic devices and sensors [3-5]. Ga<sub>2</sub>O<sub>3</sub> thin films can be prepared by several methods, for example radio frequency magnetron sputtering using gallium oxide target [6], and chemical vapor deposition using gallium tris-hexafluoroacetylacetonate as gallium source material [7]. Among these methods, radio

frequency magnetron sputtering offers the advantages of high deposition rate, low working pressure, easy control and large area film preparation. As it is well known that the processing conditions such as growth temperature and annealing conditions based on this method are critical to control the unique properties of Ga<sub>2</sub>O<sub>3</sub> thin films. Therefore, it is important to establish these processing conditions for the development of useful Ga<sub>2</sub>O<sub>3</sub> based devices [6].

Here we report the effect of annealing temperatures on the structural and optical properties of Ga<sub>2</sub>O<sub>3</sub> thin films by radio frequency magnetron sputtering method which is an example of physical vapor deposition (PVD). We show that by carefully choosing the preparation and the annealing conditions, it is possible to tune the crystallinity degree and the structural defects concentration in Ga<sub>2</sub>O<sub>3</sub> thin films.

## 2. Experimental Procedure

The Ga<sub>2</sub>O<sub>3</sub> thin films were deposited onto fused silica UV grade quartz (Inseto Limited), silicon (Si) and double polished undoped germanium (Ge) substrates using **Kurt J Lesker PVD75**. Samples preparations and sputtering conditions have been described in detail elsewhere [6]. The deposition was carried out for 16, 40 and 180 minutes for 20, 50 and 200 nm thickness, respectively (deposition rate  $\sim 0.3$  Å/s). After deposition, the thickness of the thin films was confirmed by spectroscopic ellipsometry and scanning electron microscopy (not shown). The samples were tube furnace annealed at 500, 650 and 800 °C for 30 minutes in 100 sccm N<sub>2</sub> flow.

The structure characteristics of the Ga<sub>2</sub>O<sub>3</sub> thin films deposited on Si were analysed using a Bruker D8 Advance X-ray diffractometer (XRD).

XRD patterns were recorded using  $\text{CuK}\alpha$  radiation ( $\lambda = 1.54056\text{\AA}$ ) at room temperature.

Optical transmission measurements, in the range 200-900 nm, were carried out with a double-beam UV/Vis/NIR Perkin-Elmer Lambda 9 spectrophotometer. The resolution was chosen to be at 1 nm. Infrared transmittance measurements were made with a Perkin-Elmer Frontier Fourier transform infrared (FTIR) spectrometer. The resolution was  $8\text{ cm}^{-1}$  and the scan size was 100. Samples for FTIR and UV/Vis/NIR measurements were deposited onto double polished undoped Ge and fused silica UV grade quartz substrates, respectively. All optical measurements were performed in ambient air conditions (unpurged conditions).

### 3. Results & Discussion

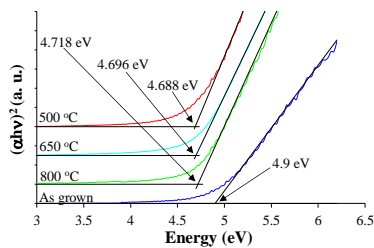
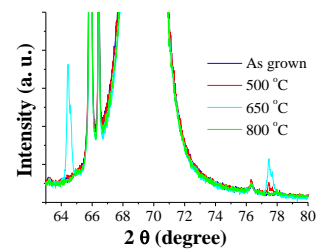


**Fig. 1** Tauc plot of 20 nm  $\text{Ga}_2\text{O}_3$  thin films before annealing and annealed at various temperatures. The spectra are offset vertically for clarity.

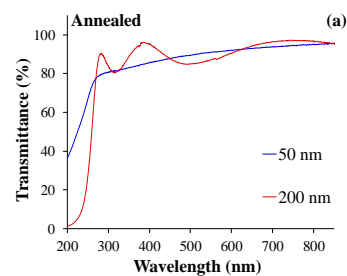
Fig. 1 shows a plot of  $(\alpha h\nu)^2$  versus photon energy (Tauc's expression) where  $\alpha$  and  $h\nu$  are the absorption coefficient and the photon energy, respectively for the as grown and 500 to 800 °C annealed 20 nm  $\text{Ga}_2\text{O}_3$  thin films. The  $E_g$  energy was estimated by extrapolating the linear part of the curves of the incident radiation to intercept the photon energy axis (at  $\alpha = 0$ ). As you can see from this figure, the  $E_g$ s shift towards lower energy after annealing indicating a change in the microscopic structure (i.e. from amorphous to crystalline) of the  $\text{Ga}_2\text{O}_3$  thin films due to the annealing process. The higher measured value of  $E_g$  for  $\text{Ga}_2\text{O}_3$  thin film before annealing may be due to excess oxygen or structural disorder induced by the amorphous nature of the thin films [6]. The increase of the optical  $E_g$  as the annealing temperature increases from 500 to 800 °C can be attributed to the decrease of defect states [8].

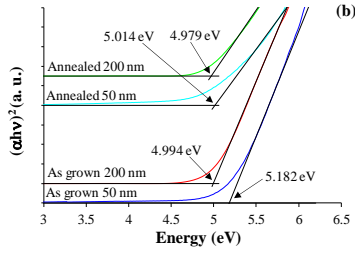
Fig. 2 shows the XRD patterns of as grown and 500 to 800 °C annealed 20 nm  $\text{Ga}_2\text{O}_3$  thin films deposited on Si substrate. The strong  $2\theta$  peak at  $\sim 69.132^\circ$  corresponds to the (0 0 4) peak of Si [9]. For the film annealed at 500 °C, a weak  $2\theta$  peak  $\sim 77.441^\circ$  corresponding to the (1010)

peak of  $\beta\text{-Ga}_2\text{O}_3$  (JCPDS 11-370) emerged, suggesting that the crystallisation process had started. Further annealing temperature increased to 650 °C results in the enhancement of this peak intensity and the appearance of a strong  $2\theta$  peak at  $\sim 64.434^\circ$ , corresponding to the (217) peak of  $\beta\text{-Ga}_2\text{O}_3$  indicating that the film has a crystalline structure [9]. With further annealing temperature increased to 800 °C, these diffraction peaks corresponding to  $\beta\text{-Ga}_2\text{O}_3$  disappeared, suggesting that the film crystallinity has degraded. This is in contrast to Fig. 1 where we attributed the increase of the  $E_g$  for  $\text{Ga}_2\text{O}_3$  thin films annealed at 800 °C to the decrease of defect states. Ramana et al [10] and Ghose et al [11] have observed similar trend of decreasing diffraction peaks from  $\beta\text{-Ga}_2\text{O}_3$  at higher temperatures. Ramana et al attributed this trend to the decrease of film thickness due to  $\text{Ga}_2\text{O}_3$  film crystallization and densification whilst Ghose et al attributed this trend to the decrease in film thickness, which result from the reduction in sticking coefficient of the  $\text{Ga}_2\text{O}$  molecules. Therefore, the absence of the diffraction peaks corresponding to  $\beta\text{-Ga}_2\text{O}_3$  at 800 °C can be attributed to the decrease of film thickness since peak intensity decreased with decreasing growth thickness and the increasing optical  $E_g$  at 800 °C is probably due to decreasing grain size with decreasing film thickness. The XRD results show that  $\text{Ga}_2\text{O}_3$  thin film annealed at 650 °C has a good degree of film crystallinity as compared to  $\text{Ga}_2\text{O}_3$  thin films annealed at 500 and 800 °C.



**Fig. 2.** XRD patterns of 20 nm  $\text{Ga}_2\text{O}_3$  thin films before annealing and annealed at various temperatures.

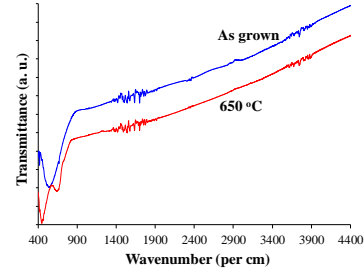




**Fig. 3** (a) Transmittance spectra of 50 and 200 nm thick Ga<sub>2</sub>O<sub>3</sub> thin films annealed at 650 °C, and (b) Tauc plot of 50 and 200 nm thick Ga<sub>2</sub>O<sub>3</sub> thin films before and after annealing at 650 °C. The spectra are offset vertically for clarity.

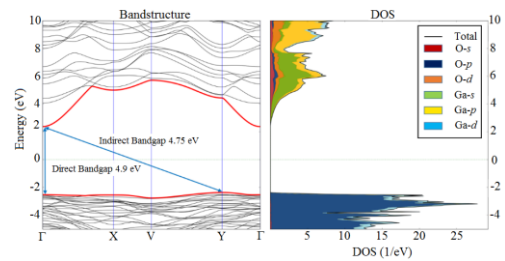
The transmittance spectra of the 50 and 200 nm thick β-Ga<sub>2</sub>O<sub>3</sub> thin films after annealing are shown in Fig. 3a. The transmittance of both samples is above 80 % in the visible and near-infrared regions and exhibits a strong absorption in the deep UV region. The 200 nm thickness curve exhibits optical thin film interference pattern and stronger absorption in the deep UV region indicating a thicker sample in agreement with spectroscopic ellipsometry and scanning electron microscopy results (not shown). In addition, we clearly observed that the absorption edge near the 250 nm wavelength red shifted towards longer wavelengths, indicating that the optical E<sub>g</sub> has decreased with increasing thickness.

Fig. 3b shows the plot of (αhν)<sup>2</sup> versus photon energy of the 50 and 200 nm thick β-Ga<sub>2</sub>O<sub>3</sub> thin films before and after annealing. Before annealing, the E<sub>g</sub> of the Ga<sub>2</sub>O<sub>3</sub> thin films were 5.182 eV and 4.994 eV for 50 nm and 200 nm, respectively. The decrease of E<sub>g</sub> with thickness can be ascribed to the increase of particle size, decrease of strain and increase of lattice constant [6]. After annealing, the E<sub>g</sub> shifts towards lower energy indicating a change in the microscopic structure (i.e. from amorphous to crystalline state) of the Ga<sub>2</sub>O<sub>3</sub> thin films due to the annealing process. This is confirmed by the absence of a broad absorption band located in the range from 400 to 900 nm<sup>-1</sup> (associated with the amorphous nature) of the as grown Ga<sub>2</sub>O<sub>3</sub> thin film and the emergence of two peaks located at 450 and 670 nm<sup>-1</sup>, which are related to the crystalline nature of annealed Ga<sub>2</sub>O<sub>3</sub> thin film as shown in Fig. 4 [12]. The experimentally measured E<sub>g</sub> values for the annealed samples ~ 4.9 eV agree reasonably with our DFT calculations (see below) indicating that the β-Ga<sub>2</sub>O<sub>3</sub> thin films are direct transition type semiconductors.



**Fig.4** FTIR transmittance spectra of 200 nm Ga<sub>2</sub>O<sub>3</sub> thin films before annealing and annealed at 650 °C. The spectra are offset vertically for clarity.

We calculated the band structures and project density of state (PDOS) for the bulk β-Ga<sub>2</sub>O<sub>3</sub> on the monoclinic cell, as show in Fig. 5. The bold red lines are the bands marked the nearest conduction band and valence band. At equilibrium, the bulk β-Ga<sub>2</sub>O<sub>3</sub> has a wide E<sub>g</sub> with 4.90 eV direct gap and 4.75 eV indirect gap at 300 K [13]. The conduction band minimum (CBM) is located at the Γ point, while the valence band maximum (VBM) is almost flat. However, the small dispersion of the VBM does not substantially affect the width of the E<sub>g</sub> because the energy difference between the direct gap and indirect gap is only 0.15 eV. In the experiment, the sharp absorption onset is around 4.90 eV, which show the bulk β-Ga<sub>2</sub>O<sub>3</sub> is a direct E<sub>g</sub> semiconductor [14]. In bulk β-Ga<sub>2</sub>O<sub>3</sub>, the O-p and Ga-d orbitals mainly contribute to the VBM whilst the CBM has contributions mainly from the Ga-s and Ga-p orbitals. The detailed procedure on using this simulation to obtain the band structures of bulk β-Ga<sub>2</sub>O<sub>3</sub> on the monoclinic cell has been outlined elsewhere [15].



**Fig. 5** The computed band structures and PDOS of the bulk β-Ga<sub>2</sub>O<sub>3</sub>.

## 4. Conclusions

A study of the transition between the amorphous and the crystallized states and their effects on the optical E<sub>g</sub>s and structural property before and after annealing has been reported. The increase of the optical E<sub>g</sub> as the annealing

temperature increases from 500 to 650 °C for the 20 nm Ga<sub>2</sub>O<sub>3</sub> thin films can be attributed to the decrease of defect states. The observed increase of the optical E<sub>g</sub> at 800 °C has been attributed to the combined effects of film thickness and the grain size decrease with increasing annealing temperatures. The XRD results show that 20 nm Ga<sub>2</sub>O<sub>3</sub> thin film annealed at 650 °C has a good degree of film crystallinity as compared to Ga<sub>2</sub>O<sub>3</sub> thin films annealed at 500 and 800 °C, indicating that there is sufficient energy for Ga<sub>2</sub>O<sub>3</sub> film crystallization at the temperature of 650 °C. It can be observed that the location of the optical absorption edge is both crystal structure and thickness dependent. The decrease of E<sub>g</sub> with thickness can be ascribed to the increase of particle size, decrease of strain and increase of lattice constant. The decreasing E<sub>g</sub> after annealing can be attributed to the increasing crystalline nature of Ga<sub>2</sub>O<sub>3</sub> films which is confirmed by FTIR spectroscopy. DFT calculations show β-Ga<sub>2</sub>O<sub>3</sub> has a direct E<sub>g</sub> of ~ 4.9 eV which is in excellent agreement with the measured values for the annealed samples indicating that the samples are β crystalline state direct E<sub>g</sub> semiconductors. The large E<sub>g</sub> and high transparency from the UV to visible wavelength make the material a potential candidate for designing next generation high power and UV optoelectronic devices.

**Acknowledgments.** The authors would like to acknowledge funding by the European Regional Development Fund, through the Welsh Government, for the 2nd Solar Photovoltaic Academic Research Consortium (SPARC II) which supported this research. The authors would like to thank J. E. Evans for his assistance with the deposition of Ga<sub>2</sub>O<sub>3</sub> thin films and C. M. Fung for the assistance with spectroscopic ellipsometry measurements.

## References

- [1] J. Millán, P. Godignon, X. Perpinà, A. Pérez-Tomás, and J. Rebollo, "A survey of wide bandgap power semiconductor devices", IEEE Trans. Power Electron., **29**(5), pp. 2155-2163, May 2014.
- [2] J. S. Park, J. K. Kim, J. Cho, and T. Y. Seong., "Review—Group III-Nitride-based ultraviolet light-emitting diodes: Ways of increasing external quantum efficiency," ECS J. Solid State Sci. Technol., **6**(4), pp. Q42-Q52, February 2017.
- [3] S. J. Pearton et al., "A review of Ga<sub>2</sub>O<sub>3</sub> materials, processing, and devices," Appl. Phys. Rev., **5**(1), pp. 011301-1-011301-53, March 2018.
- [4] X. Chen et al., "Self-powered solar-blind photodetector with fast response based on Au/β-Ga<sub>2</sub>O<sub>3</sub> nanowires array film schottky junction," ACS Appl. Mat. Interfaces, **8**(6), pp. 4185-4191, January 2016.
- [5] M. Higashiwaki, and G. H. Jessen, "Guest Editorial: The dawn of gallium oxide microelectronics," Appl. Phys. Lett., **112**(6), pp. 060401-1–060401-4, February 2018.
- [6] S. S. Kumar et al., "Structure, morphology, and optical properties of amorphous and nanocrystalline gallium oxide thin films," J. Phys. Chem. C., **117**(8), pp. 4194–4200, February 2013.
- [7] M. Passlak et al., "Ga<sub>2</sub>O<sub>3</sub> films for electronic and optoelectronic applications," J. Appl. Phys., **76**(2), pp. 686-693, January 1995.
- [8] Q. Shi et al., "Structural, optical and photoluminescence properties of Ga<sub>2</sub>O<sub>3</sub> thin films deposited by vacuum thermal evaporation," J. Lumin., **206**, pp. 53–58, February 2019.
- [9] H. W. Kim, and N. H. Kim, "Growth of gallium oxide thin films on silicon by the metal organic chemical vapor deposition method," Mater. Sci. Eng. B, **110**(1), pp. 34-37, June 2004.
- [10] C. V Ramana et al., "Chemical bonding, optical constants, and electrical resistivity of sputter-deposited gallium oxide thin films," J. Appl. Phys., **115**(4), pp. 043508-1–043508-9, January 2014.
- [11] S. Ghose et al., "Structural and optical properties of β-Ga<sub>2</sub>O<sub>3</sub> thin films grown by plasma-assisted molecular beam epitaxy," J. Vac. Sci. Technol. B, **34**(2), pp. 02L109-1–02L109-6, March/April 2016.
- [12] A. Ortiz, J. C. Alonso, E. Andrade, and C. Urbiola, "Structural and optical characteristics of gallium oxide thin films deposited by ultrasonic spray pyrolysis," J. Electrochem. Soc., **148**(2), pp. F26-F29, February 2001.
- [13] H. He, M. A. Blanco, and R. Pandey, "Electronic and thermodynamic properties β-Ga<sub>2</sub>O<sub>3</sub>," Appl. Phys. Lett., **88**(26), pp. 261904-1–261904-3, June 2006.
- [14] C. Janowitz et al., "Experimental electronic structure of In<sub>2</sub>O<sub>3</sub> and Ga<sub>2</sub>O<sub>3</sub>," New J. Phys., **13**, pp. 085014-1–085014-14, August 2011.
- [15] N. Badiei et al., "Physical, technological and electrical parameters extraction of Ga<sub>2</sub>O<sub>3</sub> thin films using combination of experimental and numerical studies," unpublished.